Adsorption and Release Kinetic Studies of Vitamin B1 Onto Halloysite Nanotubes

ADI GHEBAUR[1]*, SORINA A. GAREA[1], HORIA IOVU[1,2]

[1]University Politehnica of Bucharest,Advanced Polymer Materials Group, 1-7 Gheorghe Polizu Str., 011061, Bucharest, Romania
[2]Academy of Romanian Scientists, 54 Splaiul Independetei, 030167, Bucharest, Romania

The aim of the present work was to monitor the adsorption of thyamine hydrochloride (VB_1) onto halloysite (HNT) nanoclay in different conditions (contact time, initial pH, temperature and initial concentration). The HNT-VB_1 materials were also analyzed by FTIR, TGA, TEM and the release of VB_1 was monitored in two different simulated body fluids. Three isotherm models were used to determine the adsorption mechanism of VB_1 onto HNT. The Langmuir model showed that the adsorption process is endotherm. The Freundlich adsorption model confirms that this is a favorable process. The adsorption of VB1 onto HNT is a physical process according to Dubinin-Radushkevich isotherm. The release of VB_1 from HNT takes place by Fickian diffusion and it was monitored for 24 h. The highest amount of drug released (35%) was registered in simulated gastric fluid (pH 1.2).

Keywords: halloysite nanoclay, controlled drug release, isotherm models

A suitable procedure used for reducing the dissolution rate of drugs within the organism is the insertion of the active ingredients in micro- or nanoparticles. In order to be used in drug delivery field micro- or nanoparticles have to show a high loading capacity, high encapsulation efficiency and suitable release profile [1]. Here we may include organic and inorganic particles like magnetite, gold nanoparticles, clays, silicon nanoparticle, mesoporous silica [2-5]. Clays are inorganic layered nanoparticles that are intensively used in drug delivery in last years because present important properties like a high capacity to exchange ions and intercalate different types of biomolecules, genes, drugs, proteins within the alumino-silicate sheets. In this way the intercalated ions are protected and transported at the site of action [6]. In drug delivery field usually nanoclays are used as excipients, they favor the drug tablets disintegration [7], or they also may act as active agents due to their high specific surface area, high cation exchange capacity [8] and non-toxicity [9]. The clays used as drug delivery agents are usually natural aluminosilicates like montmorillonite, sepiolite, smectite, halloysite, bentonite, kaolinite, but also synthetic aluminosilicates like layered double hydroxide or porous clay heterostructures [10-14]. In last decade halloysite (HNT) started to be used as an active agent because it exhibits a specific surface area between 16.5-50.5 m^2/g depending by the deposit from where it is extracted [15-18]. The surface area and the inner diameter dimension of the nanotubes are two extremely important properties that influence the amount of active ingredient that may be loaded by this nanoparticles [19]. For a higher drug loading within the nanotube lumen it can be increased the inner diameter by acid etching [20]. Halloysite is a alumino-silicate with Si:Al ratio of 1:1 and have a chemical composition similar to kaolinite but with a hallow tubular structure. This is due to the poor number of hydrogen bonds caused by the water layer presence between two sheets [16]. On the internal and external surface halloysite is negatively charged but the ends are amphoteres [21]. The mathematical analysis of drug adsorption and in vitro drug release data may offer valuable informations about the mechanisms that occur within this processes. Many studies were performed in order to establish an ideal model to describe the release of drugs from porous inorganic hosts but there is no notable result. Thus, to determine the release mechanism that takes place at this level it is borrowed the Higuchi model applied at the release of drugs from porous polymeric matrix was considered [22].

In this study we examined the capacity of HNT to adsorb VB_1 from an aqueous solution. The effect of contact time, initial *p*H, temperature and initial concentration were investigated. The equilibrium data were used to determine the adsorption mechanism of VB_1 onto HNT.

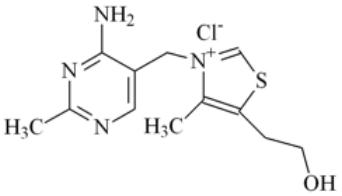

Fig. 1. Structural formula of thiamine hydrochloride

Experimental part

Materials

Thiamine hydrochloride (VB_1), and halloysite nanoclay (HNT) with a diameter of 30-70 nm, a length of 1.3 μm, a pore size volume 1.26 - 1.34 mL/g, a surface area of 64 m^2/g were purchased from Sigma Aldrich. Sodium hydroxide, potassium phosphate monobasic, hydrochloric acid, potassium chloride were received from Sigma Aldrich.

Characterization

FTIR spectra were recorded on a Bruker VERTEX 70 spectrometer using 32 scans with a resolution of 4 cm^{-1} in 4000 - 400 cm^{-1} region. The samples were analyzed from KBr pellets. Thermogravimetric analysis (TGA) was done on a Q 500 TA Instrument. The samples of 2 mg were heated from 30 to 800 °C at a scanning rate of 10 °C/min under a constant nitrogen flow rate (40 mL/min). UV-Visible absorbance of VB_1 solutions was measured at λ_{max} = 242 nm on a UV-3600 Shimadzu equipment provided with a quartz cell having a light path of 10 mm and equipped with

* email: ghebauradi@yahoo.com; Phone: (+40)214022726

a Syringe Sipper Type N. TEM images were recorded on a TECNAI F30 G^2 HRTEM equipment. The unmodified and modified halloysite were ground and sonicated in a glass vial to disperse the particles within the solvent (ethanol). The suspended particles were transferred to a copper grid (300 mesh) coated with a strong carbon film and dried in air.

Adsorption experiments

The adsorption of VB_1 from aqueous solution was performed at three different temperatures 30, 50 and 70 °C. The concentration of the non-adsorbed drug was determined by UV adsorption at 242 nm, after the centrifugation of HNT-VB_1 suspension. The amount of drug adsorbed at time t (Qt, mg/g) and at equilibrium (Qe, mg/g) were calculated with the following equations:

$$Q_t = (C_0 - C_t)V/W \quad (1)$$

$$Q_e = (C_0 - C_e)V/W \quad (2)$$

where C_0, C_t, Ce (mg/L) are the initial, t time and equilibrium concentrations of VB_1 solution; V (L) is the volume of VB_1 solution, W (g) is the mass of HNT used [23].

In vitro drug release

The drug release was performed by suspending dialysis membrane bag containing a certain quantity of HNT-VB_1 and 5 mL buffer solution of *p*H 1.2 (simulated gastric fluid, SGF) without enzymes or *p*H 7.4 (simulated intestinal fluid, SIF) without enzymes in 200 mL of the same buffer solution. Rotation speed was 100 rpm, and the temperature was kept constantly at 37°C. At intervals of 30 min, the dissolution medium was taken out and the VB_1 concentration was determined by UV absorption at 242 nm and then the analyzed solution was put back to maintain a constant volume.

Results and discussions

Characterization of HNT

FTIR Analysis

HNT exhibits two Al_2OH peaks at 3693 and 3615 cm^{-1} attributed to the OH bending that makes the connection between two Al atoms, a band at 1637 cm^{-1} assigned to the stretching vibrations of OH groups in absorbed and coordinated water, 1026 cm^{-1}, that corresponds to Si-O-Si stretching vibrations, a single Al_2OH bending band at 909 cm^{-1} [24]. The HNT-VB_1 FTIR spectrum exhibit two new peaks at 1545 cm^{-1} and 1618 cm^{-1} which are assigned to the stretching vibrations of the pyrimidine ring from drug molecules [25] (fig. 2b).

TGA results

The adsorption of VB1 onto HNT was also demonstrated by thermogravimetric analysis. In figure 3 it can be observed an increase of the total weight loss at 800°C from 16.1 % in the case of HNT to 20% for HNT-VB1. This fact is assigned to the thermal degradation of organic fraction retained by the alumino silicate.

TEM Analysis

The HNT characteristics are revealed by TEM images (fig. 4). Thus pores with a diameter of 5 nm can be observed

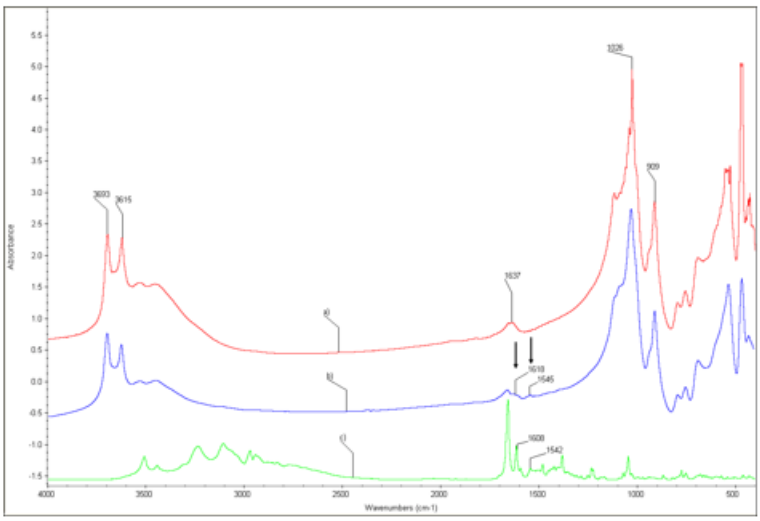

Fig. 2. FTIR spectra of: a)HNT; b) HNT-VB1; c) thiamine hydrochloride

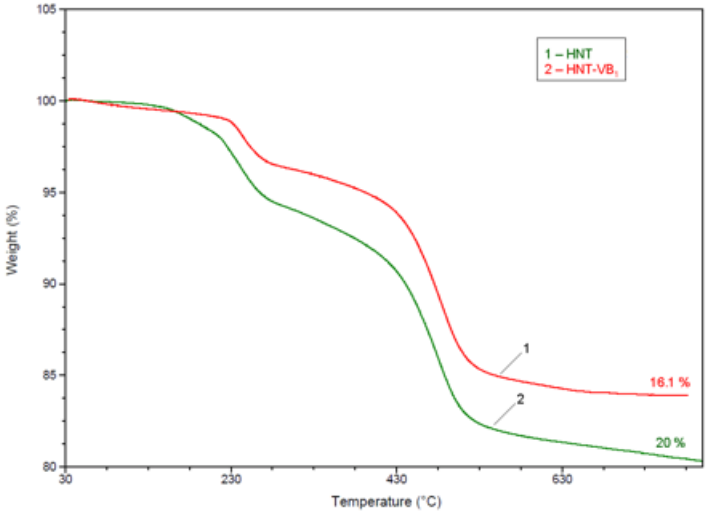

Fig. 3. TGA curves of HNT and HNT-VB1

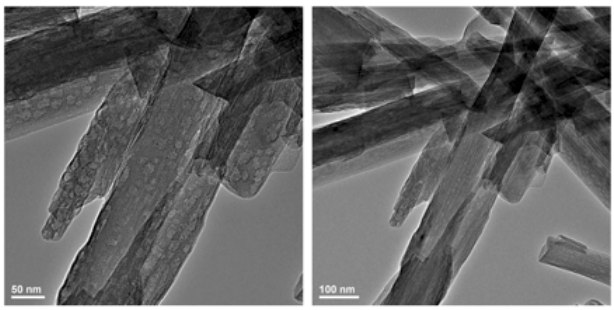

Fig. 4. HNT TEM image

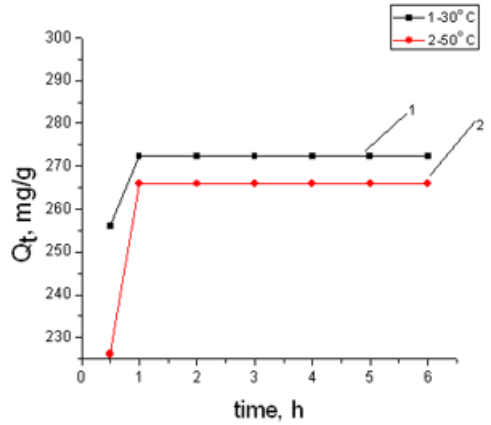

Fig. 5. The influence of contact time and temperature on the adsorption of VB1 onto HNT from aqueous solutions

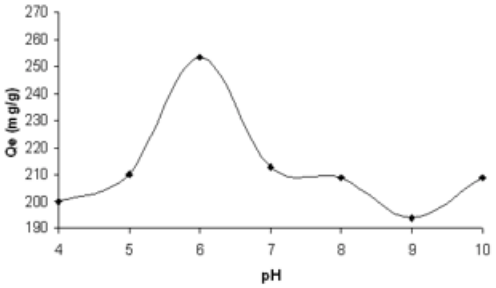

Fig. 6. The influence of *p*H on the adsorption of VB1 onto HNT; t = 30°C; reaction time = 1 h

on the surface of the nanotubes. This is important for introduction of ion metals, dyes, drugs both within the hallow tube or inside the pores located at the surface [26-28].

The influence of contact time and temperature

The effect of contact time on the adsorbed drug amount was studied using a 5g/L initial VB_1 concentration and 0.125g HNT at different temperatures (30, 50°C). From figure 5 it can be observed the influence of temperature on drug amount adsorption onto HNT. The amount of drug adsorbed at equilibrium by HNT increases at lower temperature, from 266.06 mg/g at 50°C to 272.30 mg/g at 30°C. This is probably caused by the partial degradation of VB_1 at higher temperatures [29].

The influence of pH

The effect of *p*H on the adsorbed drug amount was studied using a 5g/L initial VB_1 concentration and 0.125g HNT at different *p*H (2,3,4,5,6,7,8,9,10.5) at 30°C. The *p*H of solution was adjusted with 0.1N HCl and 0.1N NaOH. The reaction was kept under constant stirring for 1 h to reach the equilibrium. The influence of pH on the adsorption of thiamine hydrochloride onto HNT is shown in figure 6. As the *p*H increases to 6 the quantity of drug adsorbed on clay increases due to the fact that the zeta potential of HNT is negative for *p*H in the range 2-12 [27]. At pH higher than 6 the amount of drug adsorbed onto HNT decreases because unprotonated thiamine molecules are adsorbed through both nitrogen atoms from the pyrimidinic ring [16].

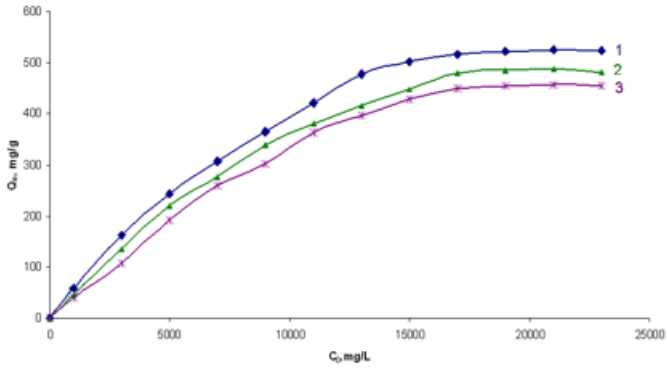

Fig. 7. The influence of initial drug concentration on the adsorption of VB1 onto HNT: 1- 30°C; 2-50°C; 3-70°C

The influence of initial concentration

The effect of initial drug concentration was studied in the range 1000-23000 mg/L using 0.125 g HNT at 30, 50, 70°C for 1 h. As it can be observed from figure 7 the adsorption capacity increases from 57.70 mg/g to 524.63 mg/g as the initial drug concentration increases at 30°C. The saturation was obtained at a concentration of 17000 mg/L.

Adsorption isotherms

In order to determine the process and mechanism of adsorption we used the adsorption isotherms models, Langmuir, Freundlich and Dubini – Radushkevich

Langmuir model

The Langmuir isotherm shows that a single adsorption layer is formed at HNT surface and it is represented by the equilibrium distribution of ions between the solid and liquid phases. So the adsorption process means the formation of a monolayer on the outer surface and after that no further adsorption takes place [30]. The Langmuir isotherm follows the next linear equation:

$$C_e/Q_e = 1/K_L Q_m + C_e/Q_m \quad (3)$$

where C_e is the concentration of VB_1 at equilibrium (mg/L), Q_e is the amount of VB_1 adsorbed by the HNT at equilibrium (mg/g), Q_m is the monolayer capacity to adsorb VB_1 (mg/g) and K_L is the Langmuir constant (L/mg). The equilibrium parameter R_L was calculated in order to determine if the process is favorable or not.

$$R_L = 1/(1+K_L C_o) \quad (4)$$

where C_0 is the highest initial VB1 concentration (mg/L). If R_L is 0 the process is irreversible, for $0<R_L<1$ the Langmuir process is favorable, for $R_L = 1$ the process is linear and if $R_L>1$ the process is unfavorable. The Langmuir parameters are shown in table 1.

A higher Q_m value is obtained at high temperature and so the adsorption process is endotherm. The values of the equilibrium parameter prove that the adsorption procecess are favorable. These results lead to the conclusion that the surface of HNT is homogenous and a monolayer of VB1 covers the surface after adsorption.

	30°C	50°C	70°C
Q_m, mg/g	714.28	769.23	833.33
K_L, L/mg	1.3410×10^{-4}	9.904×10^{-5}	7.3175×10^{-5}
R^2	0.9381	0.9702	0.9294
R_L	0.2449	0.3050	0.327

Table 1
LANGMUIR ADSORPTION PARAMETERS

Freundlich model

The Freundlich model gives information about the heterogeneous adsorbent surface. The Freundlich equation is not restricted to the formation of monolayers and is employed to describe reversible adsorption.

The linear form of Freundlich equation is:

$$\log Q_e = \log K_F + 1/n \log C_e \quad (5)$$

where K_F (mg/g(mg/L)$^{1/n}$) is the relative adsorption capacity and 1/n is the adsorption intensity parameter. To be a favorable process, Freundlich adsorption isotherm should exhibit the adsorption intensity parameter in the range $0.1 < 1/n < 1$.

As it can be observed from table 2 the values for 1/n are favorable for the system HNT-VB1 according to the Freundlich adsorption model, because 1/n is higher than 0.1 [31]. The higher values for K_F and 1/n at 30°C are in good agreement with Langmuir isotherm.

Table 2

FREUNDLICH ADSORPTION PARAMETER

	30°C	50°C	70°C
K_F, mg/g(mg/L)$^{1/n}$	0.4584	0.2181	0.1096
1/n	0.7517	0.8073	0.8881
R^2	0.9902	0.9859	0.9931

Table 3

DUBININ RADUSHKEVICH ISOTHERM PARAMETERS

	30°C	50°C	70°C
K'	-4.1801	-4.1394	-3.5341
V_m'	595.08	543.05	508.3143
E	0.3458	0.3475	0.3761
R^2	0.9795	0.987	0.9908

Dubini-Radushkevich (D-R) isotherm

Dubinin-Radushkevich isotherm gives information about the microporous systems and obeys the following linear equation [32]:

$$\ln Q_e = \ln V_m' - K'\varepsilon^2 \quad (6)$$

where V_m' is the D-R adsorption capacity (mg/g), K' is the constant related to adsorption energy (mol^2/kJ^2) and ε is the Polany potential.

$$\varepsilon = RT' \ln(1 + 1/C_e) \quad (7)$$

where R is the gas constant (kJK^{-1}mol^{-1}) and K' is the temperature (K). The free energy of adsorption (E) is calculated with the following formula:

$$E = 1/\sqrt{-2K'} \quad (8)$$

where E gives information about the physical and chemical features of adsorption.

The parameters from D-R isotherm (table 3) were determined from the plot $\ln(Q_e)$ against ε^2.

From table 3 it can observed that the calculated amount of drug adsorbed onto HNT is in good agreement with the experimental data obtained, around 524 mg/g at 30°C, 490 mg/g at 50°C and 456 mg/g at 70°C. The values for main energy of adsorption are lower than 8 kJmol^{-1} indicating that the adsorption process of VB1 onto HNT is a physical adsorption [33, 34]. Because R^2 is higher than 0.95 all the isotherms are fitted on the adsorption process of VB1 onto HNT, but Dubini-Radushkevich isotherm is better fitted.

In vitro drug release study

From figure 8 it can be noticed that the drug release profile is *p*H dependent. After 24 h only 18% of VB_1 was released from HNT-VB_1 in SIF while in SGF 35% was released. This can be due to the ion exchange process between VB_1 and the metal ions from SGF and SIF.

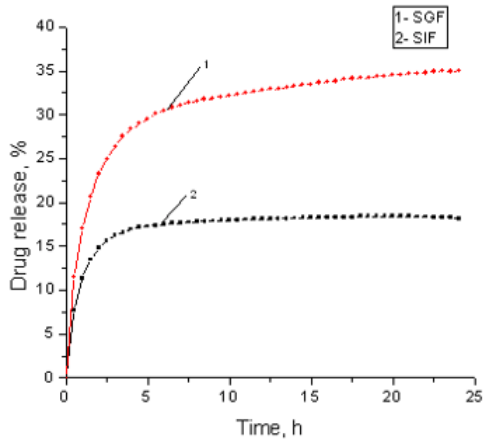

Fig. 8. Drug release profile of VB1 from HNT-VB1 system in SGF (1) and SIF (2)

In order to determine the release mechanism the obtained results were fitted by Higuchi and Korsmeyer-Peppas equations. The Higuchi model describes the release of drug as square root of time based on Fickian diffusion:

$$Q = k_H \sqrt{t} \quad (9)$$

where k_H is the Higuchi dissolution constant; Q is the amount of drug released at time t.

The Korsmeyer-Peppas derived form Fick's law and follows the equation:

$$M_t/M = kt^n \quad (10)$$

where M_t is the drug released at time t, M is the initial quantity of drug to be released, k is the kinetic constant and n is the release exponent. Based on the value of the diffusional exponent, the drug transport is classified either as Fickian diffusion (n = 0.5), non-Fickian diffusion ($0.5 < n < 1$), or Case II transport (n = 1) [35].

The release parameters determined from the two mathematical models are presented in table 4. In both cases the correlation of the parameters suggests that the release of VB1 from HNT-VB1 system takes place by Fickian diffusion.

Release media	Higuchi		Korsmeyer-Peppas		
	k_H	R^2	k	n	R^2
SGF	10.054	0.9955	10.8254	0.419	0.9701
SIF	16.035	0.9916	16.4825	0.4643	0.9881

Table 4

RELEASE PARAMETERS

Conclusions

Halloysite (HNT) is a suitable nanoclay for adsorbtion thiamine hydrochloride (VB_1) and then to release it in a proper medium. The incorporation of VB_1 molecules within the HNT structure was successfully proved by FTIR, two new peaks assigned to the stretching vibrations of the pyrimidine rings from VB_1 molecules being noticed. The adsorption of VB_1 onto HNT is also pointed out by the increase of the total weight loss from TGA tests. However it is not yet clear if the drug molecules are incorporated within the lumen of HNT or they are adsorbed mainly by the pores located at HNT surface as it is shown by TEM images. The adsorbed drug amount on HNT is influenced by the VB_1-HNT contact time, temperature and *p*H. These parameters may definitely contribute to the intensification of adsorption. Moreover the initial drug concentration plays a significant role on the adsorption process of VB_1 onto HNT. Thus a significant increase of adsorbed drug quantity is achieved as the initial drug concentration increases. However this exhibits a saturation limit of 17000 mg/L. More adsorbtion models were considered to describe the process and mechanism of adsorption. All the isotherm are fitted on the adsorbtion process of VB_1 onto HNT but Dubini-Radushkevich isotherm is the best in accuracy to fit the data. The release process of VB_1 from HNT- VB_1 systems was studied considering two mathematical models which both showed that the VB_1 release occurs by Fickian diffusion.

Acknowledgement: The work has been funded by the Sectoral Operational Programme Human Resources Development 2007-2013 of the Ministry of European Funds through the Financial Agreement POSDRU/159/1.5/S/132397.

References

1.PAGELS, R.F., PRUD'HOMME, R.K., J. Control. Release., 219, 2015, p. 519
2.CHOI, G., PIAO, H., ALOTHMAN, Z., VINU, A., YUN, C.O., CHOY, J.H., Int. J. Nanomed., 11, 2016, p. 337
3.XU, H., YAO, C., WANG, J., CHANG, Z., ZHANG, Z., Laser. Phys. Lett., 13, 2, 2016, p. 025602
4.SAGIR, T., HUYSAL, M., DURMUS, Z., KURT, B.Z., SENEL, M., ISIK, S., Biomed. Pharmacother., 77, 2016, p. 182
5.PARAMBADATH, S., MATHEW, A., BARNABAS, M.J., RAO, K.M., HA, C.-S. Micropor. Mesopor. Mat., 225, 2016, p. 174
6.SAIFULLAH, B., HUSSEIN, M.Z.B., Int. J. Nanomed., 10, 2015, p. 5609
7.SINGHAL, R.S., KENNEDY, J.F., GOPALAKRISHNAN, S.M., KACZMAREK, A., KNILL, C.J., AKMAR, P.F., Carbohyd. Polym., 72, 2008, p. 1
8.HEPPER, E.N., BUSCHIAZZO, D.E., HEVIA, G.G., URIOSTE, A., ANTON, L., Geoderma., 135, 2006, p. 216
9.CHOY, J.H., CHOI, S.J., OH, J.M., PRAK, T., Appl. Clay. Sci., 36, 2007, p. 122
10.GAREA, S.A., MIHAI, A.I., GHEBAUR, A., NISTOR, C., SARBU A., Int. J. Pharm., 491, 2015, p. 299
11.HOU, D., HU, S., HUANG, Y., GUI, R., ZHANG, L., TAO, Q., ZHANG, C., TIAN, S., KOMARNENI, S., PING, Q., Appl. Clay. Sci., 119, 2016, p. 277
12.AU, P.-I., CLODE, P., SMART, R.S.C., LEONGY.-K., Colloid. Surface. A., 484, 2015, p. 354
13.MODABBERI, S., NAMAYANDEH, A., LOPEZ GALINDO, A., VISERAS, C., SETTI, M., RANJBARAN, M., Appl. Clay. Sci., 116-117, 2015, p. 193
14.CERVINI-SILVA, J., NIETO-CAMACHO, A., RAMIREZ-APAN, M.T., GOMEZ-VIDALES,V., PALACIOS, E., MONTOYA, A., RONQUILLO DE JESUS, E., Colloid. Surface. B., 129, 2015, p. 1
15.LIU, M., GUO, B., LEI, Y., DU, M., JIA, D., Appl. Clay. Sci., 255, 2009, p. 4961
16.TARÝ, G., BOBOS, I., GOMES, C.S.F., FERREIRA, J.M.F., J.Colloid. Interf. Sci., 210, 1999, p. 360
17.TAE, J.W., JANG, B.S., KIM, J.R., KIM, I., PARK, D.W., Solid. State. Ionics., 172, 2004, p. 129
18.LI, C., JIU, J., QU, X., GUO, B., YANG, Z., J. Appl. Polym. Sci., 110, 2008, p. 3638
19.JIANG, W.-T., CHANG, P.-H., TSAI, Y., LI, Z., Micropor. Mesopor. Mat., 220, 2016, p. 298
20.LVOV, Y., WANG, W., ZHANG, L., FAKHRULLIN, R., Adv. Mater., 28, 2016, p. 1227
21.S.R. LEVIS, P.B. DEASY, Int. J. Pharm, 243, 2002, p. 125
22.VISERAS, M.T., AGUZZI, C., CEREZO, P., VISERAS, C., VALENZUELA, C., Micropor. Mesopor. Mat., 108, 2008, p. 112
23.ZHAO, M., LIU, P., Micropor. Mesopor. Mat. 112, 2008, p. 419
24.BARRIENTOS RAMIREZ, S., RAMOS FERNANDEZ, E.V., SILVESTRE-ALBERO, J., SEPÚLVEDA ESCRIBANO, A., PASTOR-BLAS, M.M., GONZALEZ MONTIEL, A., Micropor. Mesopor. Mat. 120, 2009, p. 132
25.LEOPOLD, N., CINTA PINZARU, S., BAIA, M., ANTONESCU, E., COZAR, O., KIEFER, W., POPP, J., Vib. Spectrosc. 31, 2005, p. 169
26.JINHUA, W., XIANG, Z., BING, Z., YAFEI, Z., RUI, Z., JINDUN, L., RONGFENG, C., Desalination., 259, 2010, p. 22
27.LUO, P., ZHAOA, Y., ZHANGA, B., LIU, J., YANG, Y., LIU, J., Water. Res. 44, 2010, p. 1489
28.FORSGREN, J., JAMSTORP, E., BREDENBERD, S., ENGOVIST, H., STRØMME, M., J. Pharm. Sci., 99, 2010, p. 219
29.UDEALA, O.K., ALY, S.A.S., Drug. Dev. Ind. Pharm. 14, 1988, p. 1735
30.LVOV, Y.M., SHCHUKIN, D.G., MOHWALD, H., PRICE, R.R., ACS Nano. 2, 2008, p. 814
31.ALLEN, S.J., MCKAY, G., PORTER, J.F., J.Colloid. Interf. Sci. 280, 2004, p. 322
32.GERELI, G., MURAT KUSOGLU, I., YURDAKOC, K., J.Colloid. Interf. Sci. 299, 2006, p. 155
33.JAIN, M., GARG, V.K., KADIRVELU, K., J. Hazard. Mater. 162, 2009, p. 365
34.ITODO, A.U., ITODO, H.U., Life. Sci. J., 7, 2010, p. 31
35.SCHLIECKER, G., SCHMIDT, C., FUCHS, S., EHINGER, A., SANDOW, J., KISSEL, T., J. Controlled. Release., 94, 2004, p. 25

Manuscript received: 14.03.2016